ACS OMEGA

http://pubs.acs.org/journal/acsodf

Article

Ab Initio Studies of Structural and Mechanical Properties of NH_3, NO, and N_2O Hydrates

Ningru Sun, Yanjun Li,* Nianxiang Qiu, and Shiyu Du*

Cite This: *ACS Omega* 2023, 8, 22018−22025

Read Online

ACCESS | Metrics & More | Article Recommendations | Supporting Information

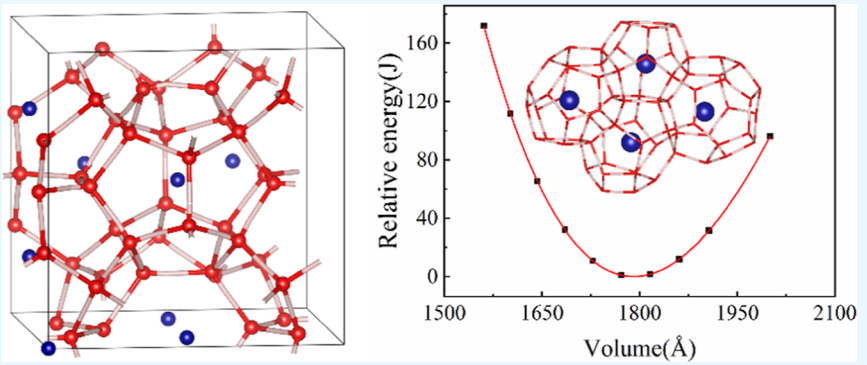

ABSTRACT: The investigation on the mechanical properties of clathrate hydrate is closely related to the exploitation of hydrates and gas transportation. In this article, the structural and mechanical properties of some nitride gas hydrates were studied using DFT calculations. First, the equilibrium lattice structure is obtained by geometric structure optimization; then, the complete second-order elastic constant is determined by energy-strain analysis, and the polycrystalline elasticity is predicted. It is found that the NH_3, N_2O, and NO hydrates all have high elastic isotropy but are different in shear characteristics. This work may lay a theoretical foundation for studying the structural evolution of clathrate hydrates under the mechanical field.

1. INTRODUCTION

Clathrate hydrates are a nonstoichiometric crystal with inclusions that forms at low temperature or high pressure.[1,2] Generally, hydrophobic gases can readily form gas hydrates, such as CH_4 and CO_2.[1] It is well-known that structures of hydrate in nature are type sI, type sII (both cubic), and sH (hexagonal) structure hydrates; the unit crystal cell of sI consists of two small cages (5^{12}) and six large cages ($5^{12}6^2$); the unit cell of sII is composed by 16 small cages (5^{12}) and 8 large cages ($5^{12}6^4$); and there are 3 (5^{12}) and 2 ($4^35^66^3$) cages and 1 large cage ($5^{12}6^8$) in sH.[1,3,4] With the discovery of a large number of undersea clathrate hydrates worldwide in the 1980s and 1990s, clathrate hydrates have become a research hotspot in the field of energy.[5,6] As an important resource, methane gas hydrate's correspondence with global climate change requires thorough inspection on its stability. Therefore, a growing number of investigations on natural gas hydrates (NGHs) have been conducted, and research direction also extends from the prevention of natural gas pipeline blockages[7,8] to resource utilization,[9−11] gas storage and transportation,[12] geological disasters,[13,14] carbon dioxide capture,[15] environmental protection,[16,17] and even gas hydrates in space.[18]

Due to the massive emissions of greenhouse gases that have caused global warming, scholars have proposed the capture and storage (CCS) of greenhouse gases.[19] Through experiments and theoretical simulation, it is finally proved feasible to use CO_2 for the replacement of CH_4 from NGHs under this storage technology. Considering the complication in geology as well as exploitation conditions for the practice of CCS with NGHs, it is necessary to determine the elasticity properties and mechanical strength of the affected greenhouse gas hydrates.[20] Moreover, this also provides requisite data in future hydrate technology to design the structures, shapes, and sizes of the transport systems accordingly. Up to now, exploration on hydrate mining and replacement is concentrated to CO_2 and organic gases, and only limited works have been carried out on the remaining greenhouse gases, which were found have the potential to extract natural gas from hydrates in the previous work.[21] Therefore, it is crucial to find the mechanical properties for different greenhouse gas components, for example, nitrogen comprises small molecules, encapsulated in gas hydrates.

Received: March 28, 2023
Accepted: May 10, 2023
Published: June 8, 2023

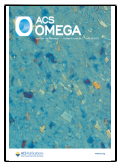

The structure and dissociation pressure of NGHs have been predicted by experiments. The ammonia clathrate was reported forming the sI hydrate.[22] Shin et al. claimed that ammonia forms clathrate hydrates and participates synergistically in clathrate hydrate formation in the presence of methane gas at low temperatures.[23] Kılıç et al. discovered that insertion of NH_3 causes serious hydrate network disturbance where the guest NH_3 molecules make H-bonds with the host water molecules.[24] For the NO gas, NO is more likely to form an sI hydrate under relatively low pressures[25] but it tends to form the sII hydrate under high pressures.[1] Hallbrucker et al. discovered that NO forms a clathrate hydrate of structure sII.[26] The N_2O hydrate has been determined as an sI structure and N_2O molecules are disordered in 5^{12} and $5^{12}6^2$.[27] The dissociation temperature of N_2O hydrates is qualitatively similar to that of CO_2 hydrates up to 110 MPa.[28−31] Sugahara et al.[29] and Yang et al.[30] claimed that N_2O molecules tend to occupy $5^{12}6^2$ of the sI structure, which is also similar to CO_2.

In recent years, the structure, nucleation and growing process, grain mechanics, and thermodynamic stability of NGHs have been predicted by theoretical calculation. For example, Jendi et al. used the first-principles method to calculate the elastic mechanical parameters of methane hydrate. Their results were consistent with previous experimental data. It was found that both methane and carbon dioxide gas hydrates exhibit high isotropy, but their shear properties differ greatly.[32] Uchida et al. used molecular dynamics (MD) simulation to calculate the bulk elastic modulus of hydrates in different ratios of CH_4 and CO_2.[20] In our previous works, we studied the microstructure and formation mechanism of different flue gases trapped in clathrate hydrates[33] and the structure and elastic properties of CH_4 and sulfide hydrates (SO_2 and H_2S) were studied by the first-principles calculation as well.[34] Fá biá et al. demonstrated that ammonia clathrate of structure sI is stable at partial filling by using Grand Canonical Monte Carlo (GCMC) simulations. In their study, they found that ammonia molecules can displace water molecules in the clathrate lattice and become incorporated into the water lattice.[22] Recently, our team used GCMC + MD to study the adsorption behavior and phase equilibrium for gas hydrates of small molecules (SO_2, H_2S, NO, and N_2O). Our results show that sulfide and nitride gases have the ability to replace CH_4 gas in NGHs. The study suggests that some flue gas components in the flue gas may contribute to the replacement of CH_4. This implies that one may save significant effort in separation of different components from flue gases when implementing replacement of CH_4 gas in NGHs with CO_2.[21,35]

Up to now, investigations on structures and properties for some hydrates like CO_2, H_2S, and SO_2 hydrates[21,34,36] have been performed, but only few inspections have been conducted on mechanical properties of hydrates encaging nitrogen-containing small molecules. This article presents a computational study on the elastic constant tensor of nitrogen-containing small-molecule hydrates from density functional theory (DFT). This work seeks to shed a light on the differences in elastic mechanical properties of three hydrates and their impact on hydrates' behavior.

2. METHODOLGY

2.1. Structure Generation. NO, N_2O, and NH_3 is small enough to form hydrate under certain pressure and temperature conditions in the sI structure.[3] The original lattice unit consists of two pentagonal dodecahedron (5^{12}) and six tetrakaidecahedron ($5^{12}6^2$) cages, totally 46 water molecules.[1] In this work, the structures of sI hydrates crystal are based on deuterated methane hydrate data from experimental high-resolution neutron diffraction measurements.[37] The hydrogen atoms in the hydrate are disordered and randomly distributed, but follow the Bernal−Fowler ice principles.[3] We assume that the occupancy rate of the cages is 100%, and there are guest gas molecules at the center of each cage.

2.2. Full Elasticity Tensor Determination. DFT is a modeling method to determine the electronic structure of the ground state. In our work, all first-principles DFT calculations are performed using the CASTEP program under the Material Studio 7.0 version.[38] The single-crystal of sI hydrates in simulations have eight cages. The convergence criteria for maximum force, maximum stress, and maximum displacement and energy are 0.01 eV $Å^{-1}$, 0.02 GPa, 5.0×10^{-4} Å, and 5.0×10^{-6}eV/atom, respectively. The energy cutoff is 400 eV. The convergence tests involved simulations with up to $2 \times 2 \times 2$ k-points. The ultrasoft form pseudopotentials are executed in the calculations. The DFT-D2 method was applied to study the effect of the long-range, dispersion van der Waals (vdW) interactions on the elastic properties. In our previous work, generalized gradient approximation (GGA) with the revised Perdew−Burke−Ernzerhof (revPBE) and the PBE functionals have been used to calculate the methane hydrate. The prediction from revPBE is found closer to the experimental measurement and other theoretical works.[34] Therefore, the revPBE functional is used in the following calculation of this work. All the atoms are relaxed during the structure optimization process. For the equations of state (EOS) fitting, the system was relaxed at different lattice parameters, and the resulting total energy was used for the fitting.

2.3. Full Elasticity Tensor Determination. In this work, we first optimize the parameters of the stable cell in the stress-free state. Then, the homogeneous finite strain method is used to calculate the complete set of second-order elastic constants (SOECs).[39] The elastic constant characterizes the material elasticity, which is the Gibbs free energy as an extension of the Taylor series with respect to the Lagrange strain. By fitting the energy−strain curve, the second-order Taylor expansion coefficient of SOECs is obtained, which is used to calculate the elastic properties of cage hydrates. First, the bulk modulus (B) and shear modulus (G) of the crystal are calculated by the Voigt−Reuss−Hill average scheme.[39] Then, Young's modulus (E) and Poisson's ratio (ν) can be derived from B and G. The SOECs are calculated from the energy variation by utilizing strains to the cubic lattice configuration. The Taylor series of elastic strain is used to represent the total energy change of the system under a zero pressure system,[40−42] In calculation, the elastic energy under strain is given by

$$\Delta E = \frac{\nu}{2}\sum_{i=1}^{6}\sum_{j=1}^{6} c_{ij}e_i e_j + O(e_i^3) \quad (1)$$

The energy increment (ΔE) is calculated by the strain with vector $\boldsymbol{e} = (e_1, e_2, e_3, e_4, e_5, e_6)$ in Voigt notation, V is the fully optimized lattice cell volume of the undistorted lattice cell, and c_{ij} is the matrix elements of elastic constants.

The original crystal lattice vector a_i (i = 1...3) is transformed into a new vector a_i' under the strain

https://doi.org/10.1021/acsomega.3c02063
ACS Omega 2023, 8, 22018−22025

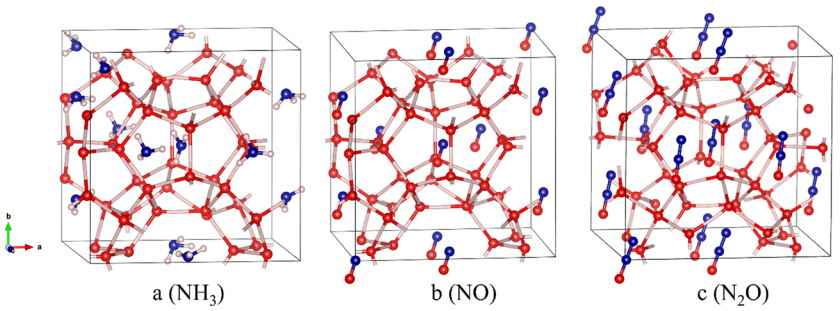

Figure 1. Crystal structures for NH_3 hydrate (a), NO hydrate (b), and N_2O hydrate (c). The oxygen, hydrogen, and nitrogen atoms are represented by red, pink, and blue balls, respectively.

$$\begin{pmatrix} a_1' \\ a_2' \\ a_3' \end{pmatrix} = \begin{pmatrix} a_1 \\ a_2 \\ a_3 \end{pmatrix} \cdot (\mathrm{I} + \varepsilon) \tag{2}$$

where ε is the strain tensor. It relates to the strain vector $\boldsymbol{e}$ by

$$\varepsilon = \begin{pmatrix} e_1 & e_6/2 & e_5/2 \\ e_6/2 & e_2 & e_4/2 \\ e_5/2 & e_4/2 & e_3 \end{pmatrix} \tag{3}$$

A volume-conserving tetragonal strain $\boldsymbol{e} = (\delta, -\delta, \delta^2/(1-\delta^2), 0, 0, 0)$ is calculated from eq 3

$$\Delta \mathrm{E} = \mathrm{V}(c_{11} - c_{12})\delta^2 + O(\delta^4) \tag{4}$$

Then, the [100] and [010] strain $e = (\delta, \delta, 0, 0, 0, 0)$ is applied which leads to

$$\Delta \mathrm{E} = \mathrm{V}(c_{11} + c_{12})\delta^2 + O(\delta^2) \tag{5}$$

Finally, c_{44} is calculated according to the shear strain e of [111], $e = (0, 0, 0, \delta, \delta, \delta)$

$$\Delta \mathrm{E} = \frac{3V}{2} c_{44} + \mathrm{O}(\delta^2) \tag{6}$$

Thus, the elastic constants (c_{11}, c_{12}, and c_{44}) are predicted according to 6 by adjusting δ as required. Equations of elastic properties are listed in the following equations.[32]

The bulk modulus (B) can be calculated from

$$B = \frac{(c_{11} + c_{12})}{3} \tag{7}$$

Shear modulus

$$G_{\mathrm{Reuss}} = \frac{5(c_{11} - c_{12})c_{44}}{4c_{44} + 3(c_{11} - c_{12})} \tag{8}$$

$$G_{\mathrm{Voigt}} = \frac{(c_{11} - c_{12} + 3c_{44})}{5} \tag{9}$$

$$G = \frac{G_{\mathrm{Voigt}} - G_{\mathrm{Reuss}}}{2} \tag{10}$$

Poisson's ratio

$$\upsilon = \frac{(3/2)B - G}{G + 3B} \tag{11}$$

Young's modulus

$$\mathrm{E} = 2G(1 + \upsilon) \tag{12}$$

Longitudinal wave speed

$$V_p = \left(\frac{B + (4/3)G}{\rho} \right)^{1/2} \tag{13}$$

Transverse wave speed

$$V_s = \left(\frac{G}{\rho} \right)^{1/2} \tag{14}$$

Zener anisotropy ratio

$$A_Z = \frac{2c_{44}}{c_{11} - c_{12}} \tag{15}$$

3. RESULTS AND DISCUSSION

3.1. Structures. Here, we calculated three type sI clathrate hydrates, i.e., NH_3 hydrates, N_2O hydrates, and NO hydrates. The crystalline structures of NH_3, N_2O, and NO hydrates are plotted in Figure 1. The lattice parameters by the EOS fitting and the fitting curve of energy versus volume for NH_3, NO, and N_2O hydrates are shown in Figure 2. The predicted lattice parameters of NH_3, NO, and N_2O hydrates are 12.095, 12.126, and 12.36 Å, respectively, which are higher than the predicted values of CH_4 hydrate (12.03 Å).[1] The lattice parameters of the N_2O hydrate can be found to be larger than those of NO and NH_3 mainly because N_2O has a larger diameter.

Analyzing the position and orientation of guest molecules can yield insights into the interactions between the host and guest molecules. For the small cage 5^{12} of sI-type hydrates, the bonds of both linear and asymmetric molecules (NO, N_2O, and NH_3) are aligned along the central axis of the water cage, which is consistent with our ab initio calculations.[33] For the cage $5^{12}6^2$, NO molecules tend to reside in off-center locations between opposite hexagons of the cages. This result is consistent with our previous report.[33] The center of N_2O is located away from the center of the equatorial plane of the $5^{12}6^2$ cages, and N_2O in the $5^{12}6^2$ cage has a long axis at an angle of approximately 30°, which is consistent with the experimental result.[27] This result is also in agreement with the results of the CO_2 hydrate reported.[43,44] The spatial disposition of guest molecules within the $5^{12}6^2$ water cages is contingent upon the symmetries of both the guest molecules and the host water cages.[27] NH_3 molecules are located near the sidewall of the water cage, and they form hydrogen bonds with water molecules.

https://doi.org/10.1021/acsomega.3c02063
ACS Omega 2023, 8, 22018−22025

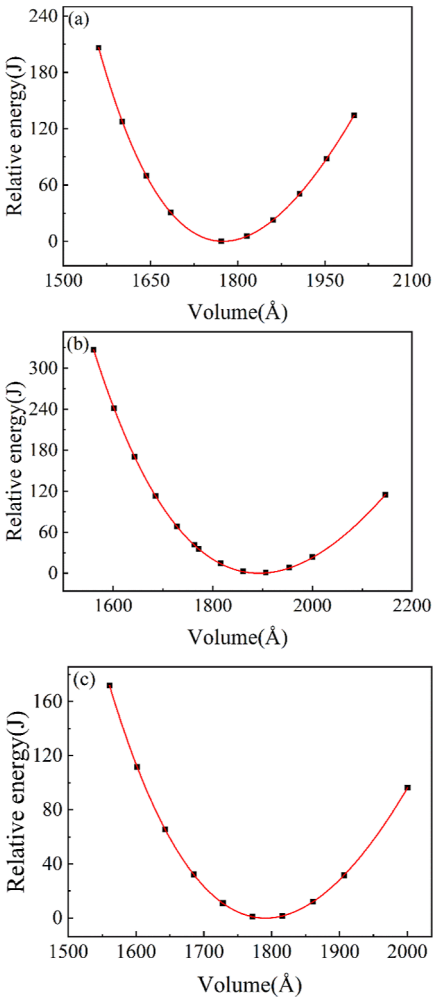

Figure 2. Energy and volume curves of (a) NH_3, (b) N_2O, and (c) NO hydrates were fitted using revPBE XC functional and Murnaghan equations, respectively.

3.2. Elastic Properties. In this work, examination on the elastic mechanical properties of NH_3, NO, and N_2O hydrates have been carried theoretically. As far as the author knows, this is the first study of the sI crystal structure of NH_3, N_2O, and NO hydrates using the first-principles calculations. The calculation results for single-crystal SOECs are given in Table 1 and all energy-strain curves are shown in Figures 3−5 for NH_3, N_2O, and NO hydrates with 100% cage occupancy. The bulk modulus of NH_3, NO, and N_2O hydrate is slightly higher than that of the methane hydrate, as shown in Table 1. On the one hand, the higher bulk modulus of NH_3 can be attributed to three hydrogen atoms per molecule, which help form multiple hydrogen bonds with water molecules,[22] and NO and N_2O are a polar molecule that increases the intermolecular interactions with the water molecules; on the other hand, unlike methane, nitrogen atoms in NH_3, N_2O, and NO are more electronegative compared with carbon atoms in methane. Also, the higher bulk modulus is consistent with the higher binding energy of NH_3 and NO compared with methane in sI hydrates.[21]

Table 1. Predicted Elastic Constant and Elastic Mechanical Properties Parameters of NH_3, N_2O, NO, and CH_4 Hydrates

elastic parameters	NH_3	NO	N_2O	CH_4[32] theory	CH_4[45,46] exp
c_{11}/GPa	17.836	19.145	18.465	18.1	11.9
c_{12}/GPa	7.247	6.499	5.050	5.7	6.3
c_{44}/GPa	5.859	8.464	9.32	6.2	3.4
ρ/g cm^{-3}	0.906	1.039	1.035	0.943	0.92
B/GPa	10.777	10.714	9.521	9.82	8.39
G/GPa	5.6261	7.531	8.170	6.23	3.54
ν	0.278	0.215	0.166	0.238	0.31
E/GPa	14.380	18.30	19.05	15.4	
V_p/Km$-^1$	4.721	4.47	4.441	4.386	3.77
V_s/Km$-^1$	2.619	2.39	2.809	2.571	1.95
A_z	1.107	1.34	1.389	0.99	1.21

In general, the elastic properties of the three hydrates are similar in many ways, with N_2O showing higher curvature in this work. The zener anisotropy factor A_Z shows that all hydrates are almost isotropic. Shimizu et al. studied the isotropy of the methane hydrate single crystals using Brillouin spectroscopy and found that the main reasons for isotropy are the rich network structure and the deviation of the perfect tetrahedral arrangement of oxygen atoms in methane hydrate.[45] Moreover, we believe that the isotropy of the hydrate is affected by the randomness of the hydrogen position in the cubic lattice. Our results show that the isotropy of nitrous oxide hydrate is slightly higher, which may be caused by the geometry or bond orientation of nitrous oxide molecules.[27]

The simulated c_{11} values have a significant difference from the experimental values of methane hydrate[45,46] in Table 1. However, compared to the theoretical value of methane hydrate, the c_{11} of N_2O and methane hydrate are similar.[32] Jendi et al. believe that c_{11} is the most sensitive parameter to the pseudopotential type, and the discrepancy with experimental results may be due to the effect of temperature, as the elastic constants significantly decrease with the temperature.[32] Regarding SOECs, N_2O and methane hydrate have an obvious difference, mainly reflected in that N_2O has larger c_{44}. The polarity of the molecule may be the cause of this phenomenon. As a polar molecule, N_2O can induce stronger intermolecular interactions with the host water molecule than methane, which can be more susceptible to structural deformation and results in a significant impact on the elastic constants. The structural characteristics of the N_2O molecule and its interaction with the host water molecule can also explain this. From a geometric point of view, it may be because the ratio of the molecular diameter to the cage diameter of N_2O hydrate is greater than that of methane hydrate, which increases the hardness of the hydrate. Interestingly, the NH_3 hydrate is predicted to be closer to the methane hydrate in both elastic constants as well as mechanical modulus than NO and N_2O. It is probably because NH_3's interaction with H_2O as both the hydrogen bond donor and acceptor allow more flexibility to adapt to the shear distortion. These results show that the encaged gas does have a remarkable effect on the mechanical behavior of the hydrate. When a shear strain takes place, it causes stronger intermolecular interaction forces change between host water and gas guest molecules since NO and N_2O are both highly polar molecules, resulting in a relatively high shear modulus; when tensile strain occurs, hydrogen atoms in NH_3 molecules is more likely to generate hydrogen bonds with hydrogen atoms in water molecules, which increases the intermolecular interaction between guest molecules and water molecules, resulting in a relatively high Poisson's ratio. It should be

https://doi.org/10.1021/acsomega.3c02063
ACS Omega 2023, 8, 22018−22025

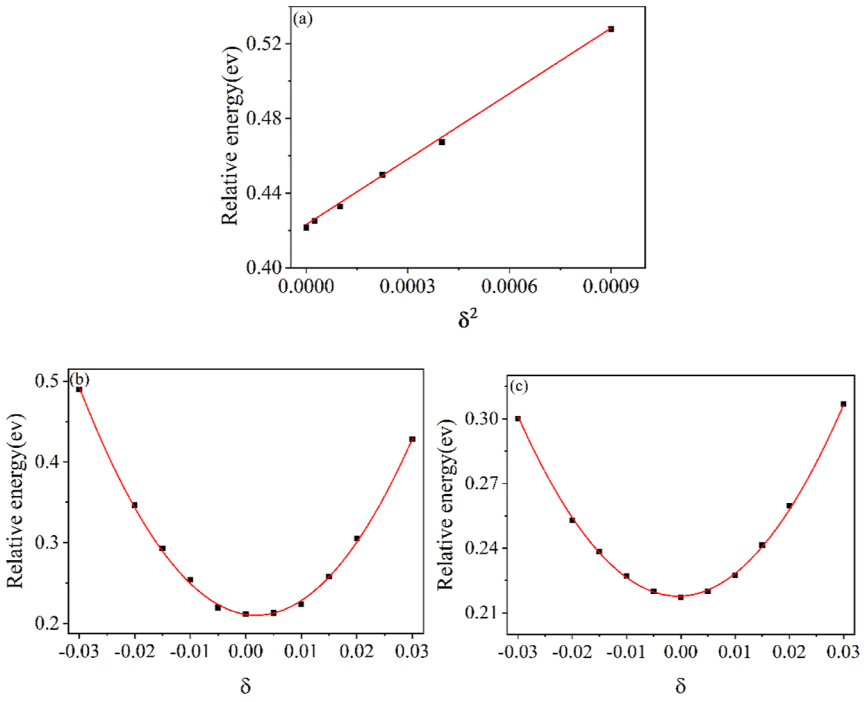

Figure 3. Strain energy density in volume-conserving tetragonal distortion (a), [100]/[010] strain (b), and shear deformation (c) for the NH_3 hydrate, respectively.

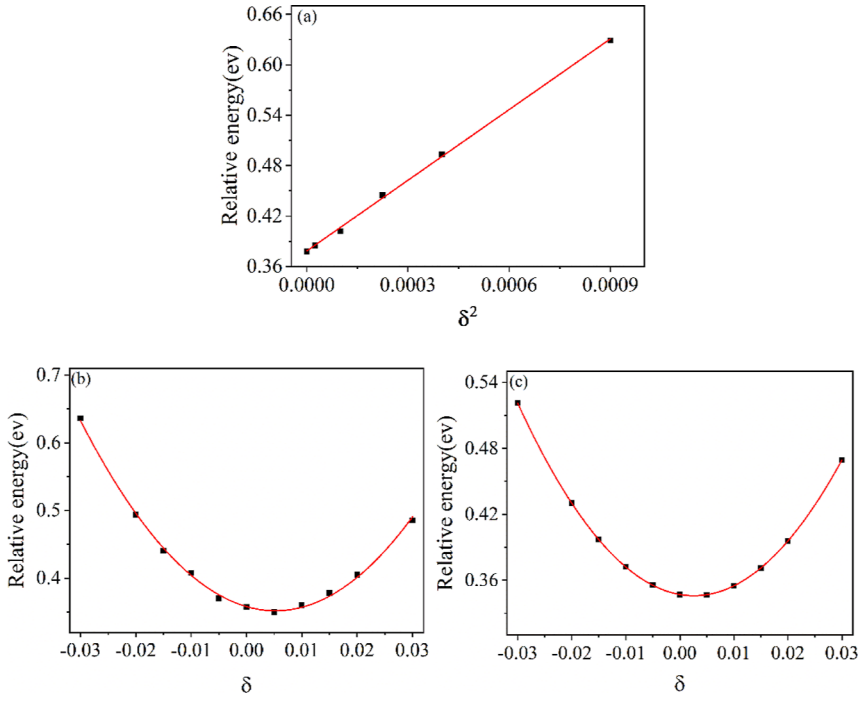

Figure 4. Strain energy density in volume-conserving tetragonal distortion (a), [100]/[010] strain (b), and shear deformation (c) for the N_2O hydrate, respectively.

mentioned that the difference between calculated and measured quantities might come from the fact that guest molecules are free to rotate in the room-temperature experiments.

It is worth mentioning that the temperature and pressure are also important factors affecting hydrates not only because too high a temperature or too low a pressure can cause the hydrate to melt but also because the chemical interaction between gas molecules and water cages might be significantly influenced. Moreover, the difference between calculated and measured quantities might come from the fact that guest molecules are free to rotate in the room-temperature experiments. Besides the current theoretical results, many other factors should be considered of the mechanical properties of hydrate which will be performed in our future work via simulations in a larger

https://doi.org/10.1021/acsomega.3c02063
ACS Omega 2023, 8, 22018−22025

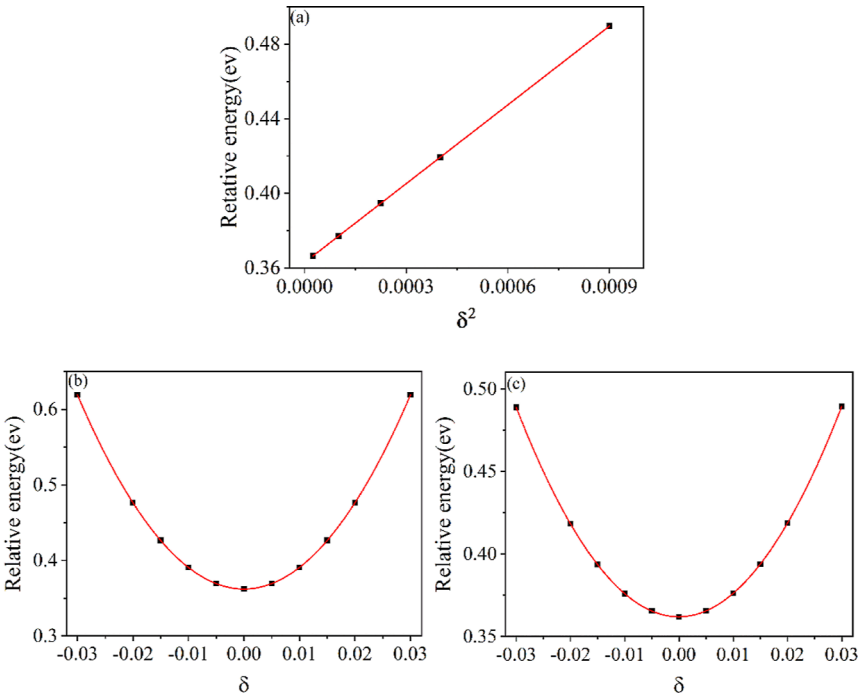

Figure 5. Strain energy density in volume-conserving tetragonal distortion (a), [100]/[010] strain (b), and shear deformation (c) for the NO hydrate, respectively.

scale in combination with more experimental results in order to build a reliable theory on clathrate hydrates.

4. CONCLUSIONS

In this article, we have presented the first-principles calculations of the structure and elastic properties of NH_3, N_2O, and NO hydrates. The elastic properties of NH_3, N_2O, and NO hydrate are analyzed by comparing with the methane hydrate. Although all hydrates are of sI-type and show high elastic isotropy, we found that there are significant differences in their shear modulus which should be further investigated for NH_3, NO, and N_2O hydrates' sequestration applications. It is expected that the elastic properties of NH_3, NO, and N_2O hydrates obtained by DFT simulation will provide a theoretical basis for the future exploitation of gas hydrate and gas storage.

■ ASSOCIATED CONTENT

Supporting Information

The Supporting Information is available free of charge at https://pubs.acs.org/doi/10.1021/acsomega.3c02063.

Crystallographic information files of NH_3, NO, and N_2O hydrates (PDF)

■ AUTHOR INFORMATION

Corresponding Authors

Yanjun Li − *College of Power and Energy Engineering, Harbin Engineering University, Harbin 150001, P. R. China*; Email: lyjhrb@126.com

Shiyu Du − *Engineering Laboratory of Advanced Energy Materials, Ningbo Institute of Materials Technology and Engineering, Chinese Academy of Sciences, Ningbo 315201, China; School of Materials Science and Engineering, China University of Petroleum (East China), Qingdao 266580, China; Milky-Way Sustainable Energy Ltd, Zhuhai 519000, China*; orcid.org/0000-0001-6707-3915; Email: dushiyu@nimte.ac.cn

Authors

Ningru Sun − *College of Power and Energy Engineering, Harbin Engineering University, Harbin 150001, P. R. China; Engineering Laboratory of Advanced Energy Materials, Ningbo Institute of Materials Technology and Engineering, Chinese Academy of Sciences, Ningbo 315201, China*

Nianxiang Qiu − *Engineering Laboratory of Advanced Energy Materials, Ningbo Institute of Materials Technology and Engineering, Chinese Academy of Sciences, Ningbo 315201, China*

Complete contact information is available at: https://pubs.acs.org/10.1021/acsomega.3c02063

Notes

The authors declare no competing financial interest.

■ ACKNOWLEDGMENTS

The present work was supported by the National Natural Science Foundation of China (grant nos. 52250005, 21875271, and U20B2021), the Entrepreneurship Program of Foshan National Hi-tech Industrial Development Zone and Zhejiang Province Key Research and Development Program (no. 2019C01060), "Pioneer" and "Leading Goose" R&D Program of Zhejiang (grant no. 2022C01236), International Partnership Program of Chinese Academy of Sciences (grant no. 174433KYSB20190019), and Leading Innovative and Entrepreneur Team Introduction Program of Zhejiang (grant no. 2019R01003)

■ REFERENCES

(1) Sloan, E. D.; Dekker, M. *Clathrate Hydrates of Natural Gases*; Elsevier, 1998.

https://doi.org/10.1021/acsomega.3c02063
ACS Omega 2023, 8, 22018−22025

(2) Moon, C.; Hawtin, R.; Rodger, P. M. Nucleation and control of clathrate hydrates: insights from simulation. *Faraday Discuss.* **2007**, *136*, 367−382.
(3) Sassen, R.; Joye, S.; Sweet, S. T.; DeFreitas, D. A.; Milkov, A. V.; MacDonald, I. R. Thermogenic gas hydrates and hydrocarbon gases in complex chemosynthetic communities, Gulf of Mexico continental slope. *Org. Geochem.* **1999**, *30*, 485−497.
(4) Pal, S.; Kundu, T. Pentagonal dodecahedron methane hydrate cage and methanol system—An ab initio study. *J. Chem. Sci.* **2013**, *125*, 379−385.
(5) Kuznetsov, A. F.; Nesterov, A. N. *Gas hydrates in permafrost*; Springer Netherlands, 2001, pp 463−486.
(6) Paull, C. K.; Ussler, W., III; Borowski, W. S.; Spiess, F. N. Methane-rich plumes on the Carolina continental rise: Associations with gas hydrates. *Geology* **1995**, *23*, 89−92.
(7) Dholabhai, P.; Englezos, P.; Kalogerakis, N.; Bishnoi, P. Equilibrium conditions for methane hydrate formation in aqueous mixed electrolyte solutions. *Can. J. Chem. Eng.* **1991**, *69*, 800−805.
(8) Gorman, A. R.; Senger, K. Defining the updip extent of the gas hydrate stability zone on continental margins with low geothermal gradients. *J. Geophys. Res.: Solid Earth* **2010**, *115*, B07105.
(9) Boswell, R. Is gas hydrate energy within reach? *Science* **2009**, *325*, 957−958.
(10) Rutqvist, J.; Moridis, G. J.; Grover, T.; Collett, T. Geo-mechanical response of permafrost-associated hydrate deposits to depressurization-induced gas production. *J. Pet. Sci. Eng.* **2009**, *67*, 1−12.
(11) Boswell, R.; Collett, T. S. Current perspectives on gas hydrate resources. *Energy Environ. Sci.* **2011**, *4*, 1206−1215.
(12) Freij-Ayoub, R.; Tan, C.; Clennell, B.; Tohidi, B.; Yang, J. A wellbore stability model for hydrate bearing sediments. *J. Pet. Sci. Eng.* **2007**, *57*, 209−220.
(13) Sultan, N.; Cochonat, P.; Foucher, J.-P.; Mienert, J. Effect of gas hydrates melting on seafloor slope instability. *Mar. Geol.* **2004**, *213*, 379−401.
(14) Garziglia, S.; Sultan, N.; Cattaneo, A.; Ker, S.; Marsset, B.; Riboulot, V.; Voisset, M.; Adamy, J.; Unterseh, S. Identification of shear zones and their causal mechanisms using a combination of cone penetration tests and seismic data in the Eastern Niger Delta. In *Submarine Mass Movements and Their Consequences*; Springer, 2010, pp 55−65.
(15) Archer, D.; Buffett, B.; Brovkin, V. Ocean methane hydrates as a slow tipping point in the global carbon cycle. *Proc. Natl. Acad. Sci. U. S. A.* **2009**, *106*, 20596−20601.
(16) Xu, W.; Lowell, R. P.; Peltzer, E. T. Effect of seafloor temperature and pressure variations on methane flux from a gas hydrate layer: Comparison between current and late Paleocene climate conditions. *J. Geophys. Res.: Solid Earth* **2001**, *106*, 26413−26423.
(17) Schmidt, G. A.; Shindell, D. T. Atmospheric composition, radiative forcing, and climate change as a consequence of a massive methane release from gas hydrates. *Paleoceanography* **2003**, *18* (1), 1004.
(18) Loveday, J.; Nelmes, R.; Guthrie, M.; Belmonte, S.; Allan, D.; Klug, D.; Tse, J.; Handa, Y. Stable methane hydrate above 2 GPa and the source of Titan's atmospheric methane. *Nature* **2001**, *410*, 661−663.
(19) Busch, A.; Amann, A.; Kronimus, A.; Kühn, M. Carbon Capture and Storage (CCS): Overview, Developments, and Challenges. *In EGU General Assembly Conference Abstracts*, 2010; p 3116.
(20) Uchida, T.; Kawabata, J. i. Measurements of mechanical properties of the liquid CO2-water-CO2-hydrate system. *Energy* **1997**, *22*, 357−361.
(21) Qiu, N.; Bai, X.; Xu, J.; Sun, N.; Francisco, J. S.; Yang, M.; Huang, Q.; Du, S. Adsorption behaviors and phase equilibria for clathrate hydrates of sulfur-and nitrogen-containing small molecules. *J. Phys. Chem. C* **2018**, *123*, 2691−2702.
(22) Fábián, B.; Picaud, S.; Jedlovszky, P.; Guilbert-Lepoutre, A.; Mousis, O. Ammonia Clathrate Hydrate As Seen from Grand Canonical Monte Carlo Simulations. *ACS Earth Space Chem.* **2018**, *2*, 521−531.
(23) Shin, K.; Kumar, R.; Udachin, K. A.; Alavi, S.; Ripmeester, J. A. Ammonia clathrate hydrates as new solid phases for Titan, Enceladus, and other planetary systems. *Proc. Natl. Acad. Sci. U. S. A.* **2012**, *109*, 14785−14790.
(24) Kılıç, M.; Devlin, J. P.; Uras-Aytemiz, N. NH_3 as simple clathrate-hydrate catalyst: Experiment and theory. *J. Chem. Phys.* **2018**, *148*, 234501.
(25) Davidson, D.; Desando, M.; Gough, S.; Handa, Y.; Ratcliffe, C.; Ripmeester, J.; Tse, J. A clathrate hydrate of carbon monoxide. *Nature* **1987**, *328*, 418−419.
(26) Hallbrucker, A. A clathrate hydrate of nitric oxide. *Angew. Chem., Int. Ed. Engl.* **1994**, *33*, 691−693.
(27) Takeya, S.; Hachikubo, A. Crystal Structure and Guest Distribution of N2O Hydrate Determined by Powder X-ray Diffraction Measurements. *Cryst. Growth Des.* **2022**, *22*, 1345−1351.
(28) Mohammadi, A. H.; Richon, D. Equilibrium Data of Nitrous Oxide and Carbon Dioxide Clathrate Hydrates. *J. Chem. Eng. Data* **2009**, *54*, 279−281.
(29) Sugahara, T.; Kawazoe, A.; Sugahara, K.; Ohgaki, K. High-Pressure Phase Equilibrium and Raman Spectroscopic Studies on the Nitrous Oxide Hydrate System. *J. Chem. Eng. Data* **2009**, *54*, 2301−2303.
(30) Yang, Y.; Shin, D.; Choi, S.; Lee, J.-W.; Cha, M.; Kim, D.; Yoon, J.-H. Cage Occupancy and Stability of N2O-Encaged Structure I and II Clathrate Hydrates. *Energy Fuels* **2016**, *30*, 9628−9634.
(31) Yang, Y.; Shin, D.; Choi, S.; Woo, Y.; Lee, J.-W.; Kim, D.; Shin, H.-Y.; Cha, M.; Yoon, J.-H. Selective Encaging of N2O in N2O−N2 Binary Gas Hydrates via Hydrate-Based Gas Separation. *Environ. Sci. Technol.* **2017**, *51*, 3550−3557.
(32) Jendi, Z. M.; Rey, A. D.; Servio, P. Ab initio DFT study of structural and mechanical properties of methane and carbon dioxide hydrates. *Mol. Simul.* **2015**, *41*, 572−579.
(33) Sun, N.; Li, Z.; Qiu, N.; Yu, X.; Zhang, X.; Li, Y.; Yang, L.; Luo, K.; Huang, Q.; Du, S. Ab initio studies on the clathrate hydrates of some nitrogen-and sulfur-containing gases. *J. Phys. Chem. A* **2017**, *121*, 2620−2626.
(34) Zong, X.; Cheng, G.; Qiu, N.; Huang, Q.; He, J.; Du, S.; Li, Y. Structures and Mechanical Properties of CH4, SO2, and H2S Hydrates from Density Function Theory Calculations. *Chem. Lett.* **2017**, *46*, 1141−1144.
(35) Qiu, N.; Bai, X.; Sun, N.; Yu, X.; Yang, L.; Li, Y.; Yang, M.; Huang, Q.; Du, S. Grand canonical Monte Carlo simulations on phase equilibria of methane, carbon dioxide, and their mixture hydrates. *J. Phys. Chem. B* **2018**, *122*, 9724−9737.
(36) Nohra, M.; Woo, T. K.; Alavi, S.; Ripmeester, J. A. Molecular dynamics Gibbs free energy calculations for CO2 capture and storage in structure I clathrate hydrates in the presence of SO2, CH4, N2, and H2S impurities. *J. Chem. Thermodyn.* **2012**, *44*, 5−12.
(37) Gutt, C.; Asmussen, B.; Press, W.; Johnson, M. R.; Handa, Y. P.; Tse, J. S. The structure of deuterated methane−hydrate. *J. Chem. Phys.* **2000**, *113*, 4713−4721.
(38) Vanderbilt, D. Soft self-consistent pseudopotentials in a generalized eigenvalue formalism. *Phys. Rev. B* **1990**, *41*, 7892−7895.
(39) Grimvall, G. *Thermophysical properties of materials*; Elsevier, 1999.
(40) Barron, T. H. K.; Klein, M. L. Second-order elastic constants of a solid under stress. *Proc. Phys. Soc.* **1965**, *85*, 523−532.
(41) Mehl, M.; Osburn, J.; Papaconstantopoulos, D.; Klein, B. Structural properties of ordered high-melting-temperature intermetallic alloys from first-principles total-energy calculations. *Phys. Rev. B* **1990**, *41*, 10311−10323.
(42) Wang, S.; Ye, H. First-principles study on elastic properties and phase stability of III−V compounds. *Phys. Status Solidi B* **2003**, *240*, 45−54.
(43) Udachin, K. A.; Ratcliffe, C. I.; Ripmeester, J. A. Structure, Composition, and Thermal Expansion of CO2 Hydrate from Single

https://doi.org/10.1021/acsomega.3c02063
ACS Omega 2023, 8, 22018−22025

Crystal X-ray Diffraction Measurements. *J. Phys. Chem. B* **2001**, *105*, 4200−4204.
(44) Alavi, S.; Dornan, P.; Woo, T. K. Determination of NMR lineshape anisotropy of guest molecules within inclusion complexes from molecular dynamics simulations. *Chemphyschem* **2008**, *9*, 911−919.
(45) Shimizu, H.; Kumazaki, T.; Kume, T.; Sasaki, S. Elasticity of single-crystal methane hydrate at high pressure. *Phys. Rev. B* **2002**, *65*, 212102.
(46) Helgerud, M.; Waite, W. F.; Kirby, S.; Nur, A. Elastic wave speeds and moduli in polycrystalline ice Ih, sI methane hydrate, and sII methane-ethane hydrate. *J. Geophys. Res.: Solid Earth* **2009**, *114*, B02212.

https://doi.org/10.1021/acsomega.3c02063
ACS Omega 2023, 8, 22018−22025